ABSTRACT

SWI/SNF ATP-dependent chromatin remodeling complexes have been related to several cellular processes such as transcription, regulation of chromosomal stability and DNA repair. The *C. elegans* gene *ham-3* (also known as s*wsn-2.1*) and its paralog *swsn-2.2* encode accessory subunits of SWI/SNF complexes. Using RNAi assays and diverse alleles we investigated whether *ham-3* and *swsn-2.2* have different functions during *C. elegans* development since they encode proteins that are probably mutually exclusive in a given SWI/SNF complex.

We found that *ham-3* and *swns-2.2* display similar functions in vulva specification, germline development and intestinal cell proliferation, but have distinct roles in embryonic development. Accordingly, we detected functional redundancy in some developmental processes and demonstrated by RNA-sequencing of RNAi-treated L4 animals that *ham-3* and *swsn-2.2* regulate the expression of a common subset of genes but also have specific targets.

Cell lineage analyses in the embryo revealed hyper-proliferation of intestinal cells in *ham-3* null mutants whereas *swsn-2.2* is required for proper cell divisions. Using a proteomic approach we identified SWSN-2.2 interacting proteins needed for early cell divisions, such as SAO-1 and ATX-2, and also nuclear envelope proteins such as MEL-28. *swsn-2.2* mutants phenocopy *mel-28* loss-of-function and we observed that SWSN-2.2 and MEL-28 co-localize in mitotic and meiotic chromosomes. Moreover, we demonstrated that SWSN-2.2 is required for correct chromosome segregation and nuclear re-assembly after mitosis including recruitment of MEL-28 to the nuclear periphery.

INTRODUCTION

Chromatin is a dynamic structure not only required for the packaging of large amounts of DNA in the limited space of eukaryotic nuclei, but also for the regulation of gene expression (HO and CRABTREE 2010; NARLIKAR *et al.* 2013). SWI/SNF complexes, which are conserved from yeast to mammals, modify the state of the chromatin in an ATP-dependent manner, and, therefore, the accessibility of distinct proteins to a given DNA region (HARGREAVES and CRABTREE 2011; EUSKIRCHEN *et al.* 2012). Such activity on the DNA regulates various cellular aspects like proliferation, differentiation, chromosomal stability, and DNA repair (REISMAN *et al.* 2009; LANS *et al.* 2010; EUSKIRCHEN *et al.* 2011). SWI/SNF complexes are involved in gene-specific regulation since only a low percentage of gene expression (6% in budding yeast, 7.5% in *Caenorhabditis elegans*) is regulated by these complexes (HOLSTEGE *et al.* 1998; RIEDEL *et al.* 2013).

A canonical SWI/SNF complex consists of a central ATPase subunit, two or three core components, and several (5 to 8) accessory subunits (HARGREAVES and CRABTREE 2011). While all SWI/SNF complexes include core subunits that are in charge of remodeling nucleosomes (PHELAN *et al.* 1999), the accessory proteins confer specificity to a given complex and their presence varies depending on the tissue and/or cellular state (WEISSMAN and KNUDSEN 2009; EUSKIRCHEN *et al.* 2012). Traditionally, SWI/SNF complexes have been classified into two subclasses, named BAF/BAP or PBAF/PBAP, depending on their signature subunits (Figure S1A). The human accessory subunits BAF60a/SMARCD1,

BAF60b/SMARCD2 and BAF60c/SMARCD3, and their worm homologs HAM-3 and SWSN-2.2 derive from the same evolutionary ancestor and are expected to belong to both subclasses of complexes (SHIBATA *et al.* 2012; WEINBERG *et al.* 2013) (Figure S1, S2). The three human BAF60 proteins, which present about 60% of similarity in their amino acid sequences, are mutually exclusive in a given SWI/SNF complex displaying distinct expression patterns and functions in humans (OH *et al.* 2008; PURI and MERCOLA 2012; JORDAN *et al.* 2013; WATANABE *et al.* 2014). BAF60c for instance, is specifically required for the transcription of myogenic-specific genes and, consequently, muscle differentiation (FORCALES *et al.* 2012). Importantly, alterations in these three BAF proteins have been associated with the progression of diverse types of cancer such as neuroblastoma, breast cancer and lung cancer (WEISSMAN and KNUDSEN 2009). Beyond cancer, mutations in SWI/SNF components contribute to the pathogenesis of other disorders, including viral infections, intellectual disability and muscular dystrophy (SANTEN *et al.* 2012; BERDASCO and ESTELLER 2013; MASLIAH-PLANCHON *et al.* 2014).

ham-3 and *swsn-2.2* are paralog genes with 67% similarity at the amino acid sequence level (Figure S3). These two genes have previously been related to several developmental processes and pathways in *C. elegans*. *ham-3* and *swsn-2.2* exhibit RNAi phenotypes in vulva development and fertility, present a synthetic genetic interaction with *lin-35*/Rb (CUI *et al.* 2004; CERON *et al.* 2007) and are implicated in somatic gonad development (LARGE and MATHIES 2014). In addition to these common functions, *ham-3* has been described to be involved in neuronal specification and in the transcriptional regulation of specific microRNAs (HAYES

et al. 2011; WEINBERG *et al.* 2013). Differently to *ham-3,* loss of s*wsn-2.2* produces Emb (embryonic lethality) and Psa (phasmid socket absent; specific cells acquiring hypodermal fate instead of the neuronal fate) phenotypes at high penetrance (SAWA *et al.* 2000; LARGE and MATHIES 2014).

Although *ham-3* and *swsn-2.2* have been associated to various developmental mechanisms, the functional interplay of the two proteins in different stages and tissues has not been formally studied. We have compiled mutant alleles for the two genes and isolated *he159*, a new allele for *ham-3*. In addition, we used RNAi to uncover functional redundancies masked by the strong phenotypes caused by null alleles. We also performed embryonic lineage analyses, RNA-sequencing, and proteomics to provide a comprehensive study of these two paralogs during development. We further investigated one of our findings to uncover a functional link between SWSN-2.2 and the nuclear envelope structure.

RESULTS

Mutant alleles for *ham-3* and *swsn-2.2*

ham-3(he159) is a novel deletion allele with phenotypes similar to other ham-3 mutants

Recently, two *ham-3* alleles, *n1654* and *tm3309*, have been described (WEINBERG *et al.* 2013; LARGE and MATHIES 2014). While *n1654* is a point mutation, *tm3309* produces a 243 bp deletion and a 4 bp insertion. Both alleles result in premature termination codons (PTCs) and presumably in the degradation of their transcripts by the Nonsense-Mediated Decay (NMD) pathway (Figure 1). We tested this assumption by Reverse–Transcription PCR (RT-PCR) with cDNA from both mutant strains and none of the *ham-3* transcripts was detected (Figure S4). Therefore, we conclude that *n1654* and *tm3309* are null alleles.

From a deletion library we isolated the novel *ham-3* allele *he159*, which consists in a 1211 bp deletion that causes a frame-shift and encodes a truncated protein (189 vs 446 amino acids (aa)) (Figure 1). The predicted protein lacks a region of 257 aa including the central SWIB domain and is only identical to the wild type protein in the first 154 aa (Figure S5). RT-PCR confirmed that the *he159* allele produces a shorter transcript (Figure S4).

All three *ham-3* alleles (*he159*, *n1654* and *tm3309*) present similar phenotypes such as short body length (Sma), egg-laying defects (Egl), adult lethality (Adl), and protruding vulva (Pvl) (Table 1, Figure S6). Due to these phenotypic similarities and the absence of the SWIB domain in the product encoded by *he159*, we conclude that *he159* most likely also represents a null mutation.

The two swsn-2.2 alleles, ok3161 and tm3395, produce truncated proteins

The *swsn-2.2* in-frame deletion allele *ok3161* lacks 1122 bp and encodes a truncated form of SWSN-2.2 (91 aa instead of 449 aa) in which the SWIB domain is absent (Figure 1 and S7). RT-PCR of *swsn-2.2(ok3161)* animals confirmed the presence of a truncated transcript (Figure S4). Though this mutation had previously been described as inviable due to larval arrest phenotype (Lva) (WEINBERG *et al.* 2013), others and we have observed homozygous *swsn-2.2(ok3161)* adult worms (LARGE and MATHIES 2014). *swsn-2.2(ok3161)* adults present dramatic levels of embryonic lethality (Figure 4A) and the F1 escaper larvae do not reach adulthood (Figure S8). Therefore, in contrast to *ham-3* alleles, *swsn-2.2(ok3161)* cannot be maintained in an unbalanced form. Homozygote *swsn-2.2(ok3161)* worms deriving from heterozygous mothers display some phenotypes that are also observed in *ham-3* alleles, such as Sma, Adl, Pvl and Egl (Table 1, Figure S6).

The second mutant allele for *swsn-2.2*, *tm3395,* has recently been characterized (LARGE and MATHIES 2014). *swsn-2.2(tm3395)* is an in-frame deletion-insertion (deletion of 421 bp and insertion of 4 bp) mutation that encodes a truncated product (Figure S4, S7). The putative truncated protein lacks 127 aa that are replaced by 3 aa but, differently from the rest of the alleles described here, the central SWIB domain is retained (Figure 1). Like *swsn-2.2(ok3161)* mutants, *swsn-2.2(tm3395)* worms display embryonic lethality and exhibit several of the phenotypes observed in *ham-3* alleles (Table 1). However, the phenotypes are

milder in *swsn-2.2(tm3395)* than in *swsn-2.2(ok3161)* animals and, as a consequence, *swsn-2.2(tm3395)* can be maintained as a homozygous strain.

In summary, mutant alleles for *ham-3* and *swsn-2.2* share some phenotypes suggesting a partial functional overlap between the two paralogs. We next investigated to what extent their functions are redundant, shared or unique during development.

ham-3 and *swsn-2.2* have redundant functions in germline and vulva development

ham-3 and swsn-2.2 function in gonad development

Both *ham-3* and *swsn-2.2* mutants display reduced brood size. We quantified the progeny of these mutants and observed temperature-dependent fertility (Figure S8). To some extent, the reduced number of progeny laid by *ham-3* and *swsn-2.2* mutants was caused by egg-laying defects (Egl) and adult lethality (Adl) (Table 1). Still, we observed that *ham-3* and *swsn-2.2* mutants have smaller germ lines (Figure S9) and, as previously reported, some mutant animals presented gonadogenesis defects including the lack of one gonad arm (LARGE and MATHIES 2014).

Since the double mutant for *ham-3* and *swsn-2.2* dies at early larval stages (LARGE and MATHIES 2014), we used RNAi to investigate whether the two genes have redundant functions in germline development. First, we constructed an RNAi clone for *swsn-2.2* since this gene was not represented in any of the two RNAi libraries available in *C. elegans* (KAMATH *et al.* 2003; RUAL *et al.* 2004). Then, we

validated the efficiency of the *ham-3* or *swsn-2.2* RNAi feeding clones by RT-PCR (Figure S10).

Started at L1 stage, double RNAi of *ham-3* and *swsn-2.2* caused a synthetic sterile phenotype due to the incapacity to produce embryos (Figures 2A and S11). These sterile animals developed smaller germ lines that were able to produce oocytes and sperm, but accumulated unfertilized endomitotic oocytes (Emo) (Figure S11).

ham-3 and swsn-2.2 act in vulval induction through the let-60/Ras pathway

The Pvl phenotype observed in *ham-3* and *swsn-2.2* mutants could be the consequence of alterations in diverse signaling pathways (Wnt, EGF and Notch) acting in Vulval Precursor Cells (VPCs) and/or uterine tissues during postembryonic development (STERNBERG 2005; GUPTA *et al.* 2012). RNAi of *ham-3* and *swsn-2.2* in wild type and mutant animals produced a genetic synthetic interaction in vulva development as the percentage of Pvl animals was synergistically higher when both genes were simultaneously inactivated (Figure 2B).

To further explore the function of *ham-3* and *swsn-2.2* in vulval induction, we performed RNAi assays in the *lin-61(n3804)*; *lin-8(n2731)* synMuv mutant, and in a *let-60*/Ras gain-of-function background (*n1046* allele*)*. Both strains display a multivulva (Muv) phenotype due to excessive induction of VPCs (STERNBERG and HAN 1998; CEOL *et al.* 2006; ANDERSEN *et al.* 2008), and *ham-3(RNAi)* and *swsn-2.2(RNAi)* enhanced the Muv phenotype in both mutant backgrounds (Figure S12). While it cannot be discarded that the two proteins are involved in more than one aspect of the regulation of vulva development, all our data indicate that *ham-3* and

swsn-2.2 act redundantly to negatively regulate the induction of VPCs. To further validate their involvement in vulva induction we used a reporter for the expression of *egl-17* (INOUE *et al.* 2002), which is a target of the Ras signaling pathway (YOO *et al.* 2004). We observed that *ham-3(RNAi)*; *swsn-2.2(RNAi)* animals show ectopic expression of *egl-17* in cells derived from the vulval precursor cells P5.p and P7.p (Figure S13). Therefore, our results indicate that the regulation of the vulval development by *ham-3* and *swsn-2.2* happens, at least to some extent, through the *let-60*/Ras pathway.

The number of postembryonic intestinal nuclei is controlled by *ham-3* and *swsn-2.2*

Since SWI/SNF complexes functionally interact with cell-cycle regulators in *C. elegans* (CUI *et al.* 2004; RUIJTENBERG and VAN DEN HEUVEL 2015), we investigated the role of *ham-3* and *swsn-2.2* in the control of the intestinal cell cycle. We took advantage of the P*elt-2*::GFP reporter to score the number of intestinal nuclei at L1 stage in *ham-3* and *swsn-2.2* mutants and observed an increase of the number of intestinal nuclei (Figure 3A). Similarly to the mutant alleles, RNAi of *ham-3* and *swsn-2.2* produced additional postembryonic intestinal nuclei (Figure 3B). This hyperproliferative effect seems to be additive when both genes are inactivated using the *ham-3(he159)* mutation in combination with *swsn-2.2(RNAi)* (Figure 3B).

Distinct and overlapping functions of *ham-3* and *swsn-2.2* in embryonic development

ham-3 and swsn-2.2 cooperate in embryonic development, but only swsn-2.2 is essential in the early embryo

The scoring of the embryonic lethality of *ham-3* and *swsn-2.2* mutants revealed a dramatic difference: while the three *ham-3* alleles produced a low percentage of dead embryos, the embryonic lethality in *swsn-2.2* mutants ranged from 80% to 100% in *swsn-2.2(ok3161)* animals (Figure 4A).

Through RNAi of *ham-3* and *swsn-2.2* we investigated whether these two genes cooperate in any embryonic developmental process. The simultaneous inactivation of these genes by RNAi starting at the L1 stage abolished the production of embryos and therefore produced sterility (Figure 4B). Thus, to study the effect of the loss of both proteins on embryonic lethality, we started the RNAi treatment in later developmental stages. Interestingly, starting at L2/L3, double RNAi of *swsn-2.2* and *ham-3* uncovered a synthetic embryonic phenotype (Figure 4B), in which embryos die at later stages than *swsn-2.2(ok3161)* embryos.

ham-3 regulates the number of embryonic intestinal cells and other Wnt-regulated embryonic processes

We analyzed the embryonic lineages of *ham-3(he159)* animals by performing 4-D video recording and lineage analyses. Interestingly, we observed that all the *ham-3(he159)* embryos analyzed (n=12) had extra cell divisions in the intestinal lineage only (Figure 5A, Figure S14). We confirmed the intestinal hyperplasia of *ham-3* mutant embryos by lineage analysis in embryos bearing the *ham-3(n1654)* allele (Figure 5A, Figure S14).

We also detected two *ham-3(he159)* phenotypes that are characteristic for mutants with defects in the Wnt signaling pathway or its effectors (CABELLO *et al.* 2010; GÓMEZ-ORTE *et al.* 2013). For instance, in one out of twelve analyzed embryos we observed a defect in the orientation of the mitotic spindle of the ABar cell at the 8-cell stage (Figure 5B) (ROCHELEAU *et al.* 1997; HERMAN 2002). The slow engulfment of apoptotic corpses was another phenotype that is shared between *ham-3(he159)* and mutants affecting the Wnt signaling (Figure 5C).

Thus, we conclude that in the embryo *ham-3* is involved in the control of the intestinal nuclei number and in the regulation of developmental processes driven by the Wnt pathway.

swsn-2.2 is required for early embryonic cell divisions

As mentioned above, the loss-of-function alleles *swsn-2.2(ok3161)* and *swsn-2.2(tm3395)* cause high rates of embryonic lethality (Figure 4A). 4-D video recording and lineage analysis of *swsn-2.2(ok3161)* embryos showed that the failure in embryogenesis occurs early in development (Files S1 and S2). The *swsn-2.2(ok3161)* embryos exhibited severe defects in early cell divisions that resulted in embryos with nuclei of different sizes (Figure 6A, 6B). Such abnormal cell division does not allow the lineage analysis later in development and causes the death of the embryo before the comma stage (Figure 6C, Files S3 and S4).

In summary, null activity of *ham-3* and *swsn-2.2* produces different embryonic phenotypes indicating specific functions. However, partial depletion of both genes

by RNAi unmasks a functional cooperation of these paralogs during embryonic development.

The identification of SWSN-2.2 interactors uncovers a functional link with the nuclear envelope

To identify potential SWSN-2.2 interactors, endogenous SWSN-2.2 was pulled-down from two biological replicates of extracts from mixed-stage worm populations. A third replicate of the experiment was performed with a synchronized population of young adult animals. As validation of our approach, mass spectrometry of the Co-IPed complexes identified several SWI/SNF subunits (Table 2). The absence of HAM-3 from any of the three replicates reflects that these two paralogs, like their human counterparts, are mutually exclusive in a given SWI/SNF complex.

In addition to several SWI/SNF subunits, we found interacting proteins required for early embryogenesis such as SAO-1 and ATX-2 (KIEHL *et al.* 2000; HALE *et al.* 2012) (Table 2, Table S1). Interestingly, we also identified nuclear envelope components, such as the nucleoporins NPP-2, NPP-9, and MEL-28 (GALY *et al.* 2003, 2006) (Table 2).

The study of the biological interactions between SWSN-2.2 and some of the potential partners identified in this work may expand the catalog of SWSN-2.2 functions. We find the interaction of SWSN-2.2 with a set of myosin-related proteins particularly interesting, since some unconventional myosins have been

related to the mitotic spindle dynamics and the regulation of gene expression (WOOLNER and BEMENT 2009; SARSHAD *et al.* 2013).

SWSN-2.2 co-localizes with MEL-28 and is required for nuclear re-assembly after mitosis and correct chromosome inheritance in the early embryo.

Since *mel-28(t1684)* and *swsn-2.2(ok3161)* mutants present similar phenotypes (adults that produce dead embryos at early stage displaying chromosomal segregation defects) (GALY *et al.* 2006), chromatin and nuclear envelope are mechanistically coupled (MATTOUT *et al.* 2015), and SWI/SNF proteins co-purify with nuclear pore proteins in mouse embryonic stem cells (HO *et al.* 2009), we decided to further investigate the functional relationship between these two genes. Taking advantage of a strain expressing GFP::MEL-28, we performed immunofluorescence to test if SWSN-2.2 and MEL-28 co-localize. In interphasic embryonic cells, SWSN-2.2 is diffusely localized in the nucleoplasm, whereas MEL-28 is present at the nuclear envelope and in the nuclear interior (Figure 7A). During mitosis, both proteins associate to chromosomes (Figure 7A). In oocytes, the two proteins localize to meiotic chromosomes and to a variable degree to the nuclear envelope, depending on the oocyte maturation stage (Figure 7B).

Finally, using the mutant *swsn-2.2(ok3161)*, we observed that SWSN-2.2 is required for nuclear re-assembly after mitosis and for the recruitment of MEL-28 to the nuclear periphery in the early embryo and in the adult germline (Figure 8, S15). On the contrary, *ham-3(he159*) animals did not show any of these embryonic

defects (Figure 8). This further supports that *ham-3* and *swsn-2.2* have distinct functions in the early embryo.

Transcriptomic analyses identify common and specific targets of HAM-3 and SWSN-2.2

Finally, to further explore the common and distinct functions of *ham-3* and *swsn-2.2*, the transcriptomes of L4 animals fed with *ham-3(RNAi)* or *swsn-2.2(RNAi)* for 36h at 25°C were compared with that of a control population fed with *gfp(RNAi)*. The reason to choose L4 stage for this experiment was that somatic and germline genes could be targeted. Beyond that stage, some animals die during the reproductive phase in response to *ham-3(RNAi)* and *swsn-2.2(RNAi).* At the stage in which the animals were harvested they begin to display the Protruding Vulva phenotype.

We detected a significant overlap (p≤0,0001, Chi-square test) between genes up- or down-regulated in *ham-3(RNAi)* and *swsn-2.2(RNAi)* animals. Thus, we identified 183 genes that may be co-regulated (69 repressed and 114 activated) by both HAM-3 and SWSN-2.2 (Figure 9A, Table S2), suggesting that either paralog could be present in the complexes that control the expression of those genes. In addition we found genes whose expression seems to be preferentially affected by one of the two paralogs. The number of genes activated or repressed in *ham-3(RNAi)* and in *swsn-2.2(RNAi)* worms suggests that HAM-3 has a major role in gene activation whereas SWSN-2.2 is preferentially involved in gene repression (Figure 9A). We performed GO terms analyses and found that HAM-3 and

SWSN-2.2 function on diverse general biological processes (Figure S16). The influence of both genes in the immune system process is particularly interesting since it has been demonstrated that SWI/SNF proteins physically interact with DAF-16 to regulate DAF-16 targets (RIEDEL *et al.* 2013), and DAF-16 itself is the effector of the Insulin/IGF-1 Signaling (IIS) pathway that is involved in the innate immune response (JENSEN *et al.* 2010).

We investigated whether there is an overlap between HAM-3 and SWSN-2.2 regulated genes and a list of DAF-16 targets (PINKSTON-GOSSE and KENYON 2007) and we found a significant number of DAF-16 targets amongst the genes activated or repressed by *ham-3* and *swsn-2.2* (Figure 9B). We further analyzed our RNA-seq data searching for genes deregulated in *daf-16* and *swsn-1* young adult mutants (RIEDEL *et al.* 2013). Although our transcriptomic study was performed at L4, we found that ≈20% of the HAM-3 and SWSN-2.2 targets are also deregulated in *daf-16* and/or *swsn-1* mutants (Figure S17).

In summary, HAM-3 and SWSN-2.2 influence the transcriptional activity of common genes but also have specific targets. This is in agreement with the overlapping and distinct roles that we describe during development. The differential occupancy of promoter regions of DAF-16 targets suggested by our study, however, needs further investigation by ChIP-sequencing.

DISCUSSION

In cancer, as in other diseases, SWI/SNF genes are found inactivated in multiple manners. Mutations in these genes can be somatic or originated in the germline and produce loss-of-function to different extents. Besides deletions and point mutations, DNA rearrangements and epigenetic marks can modify SWI/SNF activities (SHAIN and POLLACK 2013; ROMERO and SANCHEZ-CESPEDES 2014). In our study we analyzed the consequences of the inactivation of two SWI/SNF paralogs by diverse mutations and RNAi. *ham-3* and *swsn-2.2* double mutants are not viable, but RNAi allows the modulation of loss-of-function effects and thereby the uncovering of new functional relations. Thus, only by RNAi was possible to identify a functional redundancy between *ham-3* and *swsn-2.2* in fertility, vulval induction and embryonic development. The synthetic phenotypes between SWI/SNF subunits help understand the function of these chromatin remodelers in different processes, but also present an opportunity for therapies (HELMING *et al.* 2014). Nowadays, the emerging CRISPR/Cas9 approaches to edit the genome might fuel the investigation of functional interactions between specific loss-of-function mutations of SWI/SNF genes (FRØKJÆR-JENSEN 2013).

Redundant, shared and unique functions

Functions of SWI/SNF subunits have been catalogued as redundant, shared or unique (BEZHANI *et al.* 2007). Others and we have found these three modes of interaction between *ham-3* and *swsn-2.2*. While *swsn-2.2* has a unique function in early embryonic cell divisions, only *ham-3* affects the development of the

hermaphrodite specific neurons (HSNs) (DESAI *et al.* 1988; WEINBERG *et al.* 2013). Since the HSNs stimulate the vulva muscle cells to extrude embryos, the high penetrance of the Egl phenotype in animals where *ham-3* was inactivated can be explained by this neuronal defect.

We found that *ham-3* and *swsn-2.2* act redundantly in developmental processes such as germline or vulva development. This redundancy implies that either HAM-3 or SWSN-2.2 can be part of the SWI/SNF complexes regulating these processes.

Finally, a shared function is assigned when the simultaneous inactivation of both genes does not cause a clear synthetic phenotype, suggesting regulation by more than one SWI/SNF complex. Our data suggests that the control of the intestinal cell number could be a function shared by HAM-3 and SWSN-2.2.

Role in germline development

Double inactivation of *ham-3* and *swsn-2.2* by RNAi produces endomitotic oocytes (Emo phenotype) resulting in sterility. The Emo phenotype can be caused by defects of the somatic gonad that block the maturation signals to oocytes (MCCARTER *et al.* 1997). Since BAF and PBAF complexes have previously been related to *C. elegans* somatic gonad development (CUI *et al.* 2004; SHIBATA *et al.* 2012; LARGE and MATHIES 2014), HAM-3 and SWSN-2.2 could be involved in the onset of somatic gonad precursors (SGPs) as well as in the differentiation of the cells derived from these SGPs. In fact, *ham-3* and *swsn-2.2* have been identified as enhancers of the *ehn-3(rd2)* mutation, which is a mild allele of a gene specifically expressed in SGPs and required for the correct development of the

somatic gonad (LARGE and MATHIES 2014). The somatic gonad influences germ cell proliferation, which may explain the reduced germ cell number observed when *ham-3* and *swsn-2.2* activities are inhibited (KIMBLE and CRITTENDEN 2005; KORTA and HUBBARD 2010). Given the functional relationship between SWI/SNF complexes and DAF-16, another way for HAM-3 and SWSN-2.2 to play a role in fertility is through the control of germline proliferation orchestrated by the Insulin signaling pathway in somatic tissues (MICHAELSON *et al.* 2010; QI *et al.* 2012). Still, a direct function of *ham-3* and *swsn-2.2* in germ cell proliferation cannot be discarded.

Role in vulva development

We have demonstrated that during postembryonic development *ham-3* and *swsn-2.2* inhibit the induction of the vulva by acting, at least partially, through the *let-60*/Ras pathway. The Zinc-finger protein SOMI-1 binds the promoter of *let-60* to repress its gene expression and therefore inhibit the induction of the vulval precursor cells (VPCs) (HAYES *et al.* 2011). Hayes and coworkers described that HAM-3 cooperates with SOMI-1 in the differentiation of hypodermal cells (HAYES *et al.* 2011). Therefore, a direct inhibitory action of HAM-3, and maybe of SWSN-2.2, on the promoter of *let-60* could explain their role in repressing vulva induction. Moreover, considering that *ham-3* genetically interacts with *lin-35*/Rb (CERON *et al.* 2007), which is a synthetic Multivulva class B gene (synMuv B genes produce a multivulva phenotype when a synMuv A or C gene is inactivated in parallel), we cannot discard a role for *ham-3* and *swsn-2.2* in the synMuv pathway that also represses the induction of the vulva (FAY and YOCHEM 2007).

Cell cycle control

A recent study in *C. elegans* has shown that cell cycle inhibitors and SWI/SNF subunits regulate the cell cycle exit (RUIJTENBERG and VAN DEN HEUVEL 2015). Our lineage analyses of *ham-3* loss-of-function alleles showed an increase of the intestinal cell number due to extra cell divisions during embryogenesis. This additional round of intestinal cell division indicates a misregulation of the cell cycle exit and mimics the embryonic phenotypes caused by *cki-1* loss-of-function mutations rather than those of *cdc-25.1* gain-of-function mutants where cells divide much faster (CLUCAS *et al.* 2002; KOSTIĆ and ROY 2002). This fact, and the somatic gonad phenotypes caused by the inactivation of *cki-1* (KOSTIĆ *et al.* 2003; FUJITA *et al.* 2007) suggest that *ham-3*, *swns-2.2* and the G1/S inhibitor *cki-1* may be functionally related in more than one developmental process.

SWSN-2.2 and the nuclear envelope in the early embryo

Concurrently with previous publications, we observed that inactivation of *swsn-2.2* results in embryonic lethality (SAWA *et al.* 2000; LARGE and MATHIES 2014). In addition, we found that SWSN-2.2 localizes to mitotic chromosomes of early embryonic cells, which is consistent with the aberrant pattern of cell divisions observed in *swsn-2.2(ok3161)* mutants. Consistently, other SWI/SNF subunits have been found associated with chromosomes of diverse postembryonic cell types in *C. elegans* (SHIBATA *et al.* 2012).

We found protein-protein interactions between SWSN-2.2 and nuclear pore proteins. Nuclear pore proteins also copurify with SWI/SNF factors in mouse

embryonic stem cells (HO *et al.* 2009). However, although it is accepted that chromatin and nuclear envelope are mechanistically coupled (MATTOUT *et al.* 2015), it is quite speculative how components of both structures coordinate their functions. siRNA knockdown of the SWI/SNF core component BRG1 produces nuclear shape changes (IMBALZANO *et al.* 2013). Thus, the interaction between SWSN-2.2 and nuclear envelope proteins helps to understand the nuclei of different sizes observed in *swsn-2.2(ok3161)* embryos.

We observed that SWSN-2.2 and MEL-28 colocalize on mitotic chromosomes in the early embryo. The nuclear envelope breaks down and re-establishes during every round of the cell cycle, and MEL-28 is required for this process in the *C. elegans* embryo. During interphase MEL-28 is associated with nuclear pore complexes, but it is present at the kinetochores at the onset of mitosis and on chromatin in late mitosis, where it is required for the correct segregation of the chromosomes and for nuclear pore complex assembly (FERNANDEZ and PIANO 2006; GALY *et al.* 2006). Similarly to *swsn-2.2(ok3161)* mutants, inactivation of *mel-28* causes changes in nuclear morphology and abnormal distribution of nuclear pore complexes. We have shown that SWSN-2.2 is not only involved in chromosome segregation but also necessary for the recruitment of MEL-28 to chromatin to induce nuclear re-assembly after mitosis.

Therefore, the interaction between SWNS-2.2 and MEL-28 is physical and functional. *swns-2.2* was not found as one of the *mel-28* interactors during postembryonic development in *C. elegans* (FERNANDEZ *et al.* 2014), suggesting that their functional interaction may occur only at specific developmental stages.

In this study we show how during embryonic development SWSN-2.2, but not its paralog HAM-3, is required for the proper formation of the nuclear envelope. A recent RNAi-based study of chromatin regulators during *C. elegans* embryogenesis suggests the existence of at least two functionally distinct SWI/SNF complexes in the early embryo (KRÜGER *et al.* 2014), supporting the different implications of HAM-3 and SWSN-2.2 in embryonic development demonstrated in our work.

SWI/SNF proteins and the IIS pathway

SWI/SNF proteins physically interact with the transcription factor DAF-16/FOXO to regulate the expression of DAF-16 targets (RIEDEL *et al.* 2013). Stress conditions diminish the insulin signaling and increase the amount of nuclear DAF-16. In agreement with a functional correlation between SWI/SNF proteins, DAF-16 and stress, BAF SWI/SNF complexes have been shown to be involved in the stress response through the IIS pathway (KUZMANOV *et al.* 2014). However, in the absence of stress, we also found that many genes regulated by *ham-3* and *swsn-2.2* were DAF-16 known targets, which might reflect primarily the presence of HAM-3 and SWSN-2.2 in the promoter region of such DAF-16 regulated genes. Therefore, while SWI/SNF complexes were described to bind predominantly genes activated by DAF-16 under stress conditions (RIEDEL *et al.* 2013), we found that HAM-3 and SWSN-2.2 may also have a role in activation and in repression of DAF-16 targets in the absence of stress. ChIP experiments should not only determine to what extent these accessory subunits overlap with DAF-16 binding

sites but also identify genes specifically and differently regulated by HAM-3 or SWSN-2.2.

We have demonstrated that HAM-3 and SWSN-2.2 could have common and specific impact on diverse cancer-related processes such as the control of the cell cycle or cell division. Moreover we have related these two SWI/SNF subunits with cancer-related pathways such as Ras or Wnt. The tissue specificity and the synthetic phenotypes reported for these SWI/SNF accessory subunits should encourage deeper research due to their potential for future therapies.

ACKNOWLEDGMENTS

Some strains were provided by the CGC (Caenorhabditis Genetics Center), which is funded by NIH Office of Research Infrastructure Programs (P40 OD010440). IE was granted with an IDIBELL PhD fellowship. JC is a Miguel Servet Researcher (ISCIII). This study was supported by a grant from the Instituto de Salud Carlos III (ISCIII) (Ref. PI12/01554), which is cofunded by FEDER funds/European Regional Development Fund (ERDF)—a way to build Europe. PA laboratory was supported by funding from MINECO (Ref. BFU2013-42709-P).

MATERIAL AND METHODS

Strains and Maintenance

Standard methods were used to culture and manipulate worms (STIERNAGLE 2006). Wild type strain Bristol N2 and the following mutant and reporter strains were used: BN311 *bqIs311* [*gfp::mel-28*] II, CER30 *ham-3(he159)* III/hT2 (I,III); rtIs18[P*elt-2::gfp*] I, CER31 *swsn-2.2(ok3161)* I/hT2 (I,III); rtIs18[P*elt-2::gfp*] I; CER123 *ham-3(he159)* III/hT2 (I;III), HA661 rtIs18[P*elt-2::gfp*] I, MT2124 *let-60(n1046)* IV, MT3971 *ham-3(n1654)* III, RA440 *swsn-2.2(tm3395)* I/hT2 (I;III), RA459 *ham-3(tm3309)* III/hT2 (I;III), VC2789 *swsn-2.2*(*ok3161*) I/hT2 (I;III), MT12839, *lin-61(n3809)* I; *lin-8(n2731)* II; PS3972 *unc-119(ed4) syIs90* [*egl-17::*yfp + unc-119(+)] III.

RNA-mediated interference (RNAi)

RNA-mediated interference (RNAi) by feeding was performed on NGM plates supplemented with 50 µg/ml ampicillin, 12.5 µg/ml tetracycline, and 3 mM IPTG. RNAi clones were validated by PCR and/or sequencing. Synchronized L1 populations were seeded on the RNAi clones and incubated at 20°C or 25°C. The RNAi clone for *ham-3* was taken from the ORFeome library. In the case of *swsn-2.2* no RNAi clone was available. To generate one, cDNA of N2 animals was used as template and PCR using specific primers for *swsn-2.2* was performed. Using the MultiSite Gateway Vector Construction Kit, the insert was cloned into the pGC49 vector and transformed into the bacterial strain DH5α. Once amplified and purified, the plasmid was transformed into the definitive bacterial host strain HT115.

Video recording and lineage analysis

Embryos used for the lineage analysis described in this work were prepared and mounted as described by Sulston et al (SULSTON *et al.* 1983). Gravid hermaphrodites were dissected and two- to four-cell-stage embryos were mounted on 4% agar pads in water and sealed with Vaseline. 4D microscopy (3D of the embryo + time) was carried out using a multifocal plane, time-lapse recording

system. The device was based on a Leica DM 6000 microscope fitted with Nomarski microscopy. Recordings were made using a 100X/1.4 PL APO objective and the temperature was kept constant at 25ºC. The microscope was controlled with the open-source software Micro-manager. Pictures from 30 focal planes (1 µm/section) were taken every 30s for up to 12h. The SIMI Biocell software allowed tracing of the cell lineage of the embryos in time and space as well as tracing of the mitoses and apoptosis. Lineages of apoptotic cells were followed until the onset of the dead cell, and then the corpse was followed until it was engulfed and disappeared, as described in Nieto et al. (NIETO *et al.* 2010).

Immunofluorescence

Gonads were dissected and fixed in a glass multi-well plate (Pyrex® Plate, Cat. No. 71563-01) as described in Fontrodona et al (FONTRODONA *et al.* 2013). For blocking, the fixed gonads were incubated with PBS-Tween + 0.1% BSA for 1h at RT. Incubation with primary antibodies was performed at 4°C o/n, and incubation with secondary antibodies for 2h at RT. Gonads were counter-stained with DAPI included in mounting media. Immunostaining of embryos was performed following the Freeze-Crack protocol (ASKJAER *et al.* 2014). Q5536 is a polyclonal antibody generated upon our request against the first 89 amino acids of the N-terminal of SWSN-2.2. Antibodies were used at the following dilutions: anti-SWSN-2.2 (SDIX, Q5536; 1:500), anti-GFP (Molecular Probes, A11120, 1:200), anti-MEL-28 (BUD3; 1:250), mAb414 (Covance MMS-120R; 1:250), anti-rabbit (Abcam, Alexa Fluor® 568; 1:500), anti-mouse (Abcam, Alexa Fluor® 488; 1:500).

RNA-Sequencing

RNA from *gfp(RNAi)*, *ham-3(RNAi)* and *swsn-2.2(RNAi)* L4 animals was isolated with TRIReagent and purified by using the Purelink RNA Mini kit (Ambion) and DNAse I (Ambion). Quality of RNA samples was analyzed on the Agilent 2010 Bioanalyzer. Samples were multiplexed in libraries for RNA-Sequencing on Illumina Hiseq 2000 platform, through the CNAG (Centre Nacional d'Anàlisi Genòmica) sequencing facility at the Barcelona Parc Científic. More than 50

millions of reads for sample were mapped against the *C. elegans* worm version WS236 following GEMTools pipeline (http://gemtools.github.io/). The resulting BAM files were analyzed using SeqSolve software, which use Cufflinks/Cuffdiff for differential gene/transcript expression analyses (TRAPNELL *et al.* 2012). The sequence data for the three transcriptomes analyzed in this study is available at the NCBI Gene Expression Omnibus (http://www.ncbi.nlm.nih.gov/geo/) under accession number GSE75703.

Co-immunoprecipitation and Mass spectrometry

For immunoprecipitation, the Dynabeads®Co-immunopreciptation Kit was used. The included IP buffer was modified with 100mM NaCl, and protease and phosphatase inhibitors. Mixed populations or synchronized young adult N2 animals were harvested, washed with the modified IP buffer and added dropwise into liquid nitrogen to produce worm-pearls. These pearls were grounded to a fine powder in liquid nitrogen using a pestle and mortar, and allowed to thaw on ice. By centrifugation solid particles were separated from the protein extract. Antibody-conjugated beads were prepared using 2mg of Dynabeads and 10µg of antibody per reaction. The antibodies used were: anti-SWSN-2.2 (Q5536); unspecific anti-rabbit (TEBU-BIO, 036SC-2027). For immunoprecipitation, 3 mg of total protein was brought to a volume of 1ml with modified IP buffer. 1.5 mg antibody-conjugated beads were added to the protein sample and incubated for 20 min at 4°C under rotation. Subsequent washing steps were performed according to the manufacturer´s instructions.

For mass spectrometry, complexes were eluted by resuspending the beads for 30s in 50µl Glycin pH 2.5, followed by neutralization with 5µl Tris-HCl pH 10.4. Complexes were precipitated with ice cold acetone o/n. Pellets were resuspended with 6M Urea/200mM NH4HCO3, and digested with Trypsin. Then 45% of the CoIP samples and 0.5% of the Input were injected in an Orbitrap XL. BSA controls were included both in the digestion and LC-MS/MS analyses for quality control. The data was analyzed using an internal version of the search algorithm Mascot (www.matrixscience.com) against a NCBI_Celegans (February 2014) database. Peptides were filtered based on peptide score. The protein/peptide

identification information was obtained from Proteome Discoverer software (v1.4.1.14).

RT-PCR

Synchronized worm populations were harvested, frozen in TRI Reagent® and total RNA isolated using standard methods. To eliminate DNA contaminations, the DNAse I Amplification Grade system (Invitrogen™) was used. cDNA was synthesized with oligo(dT) primers using the RevertAid H Minus First Strand cDNA synthesis kit (Thermo Scientific) following the manufacturer's instructions. Semiquantitative PCR was performed using the BIOTAQ™ PCR Kit. For the quantification of gene expression levels, the Roche LightCycler 480 Instrument I and SYBR green I Master Kit were used. Gene expression was normalized to transcript levels of the housekeeping gene *act-1*.

FIGURES

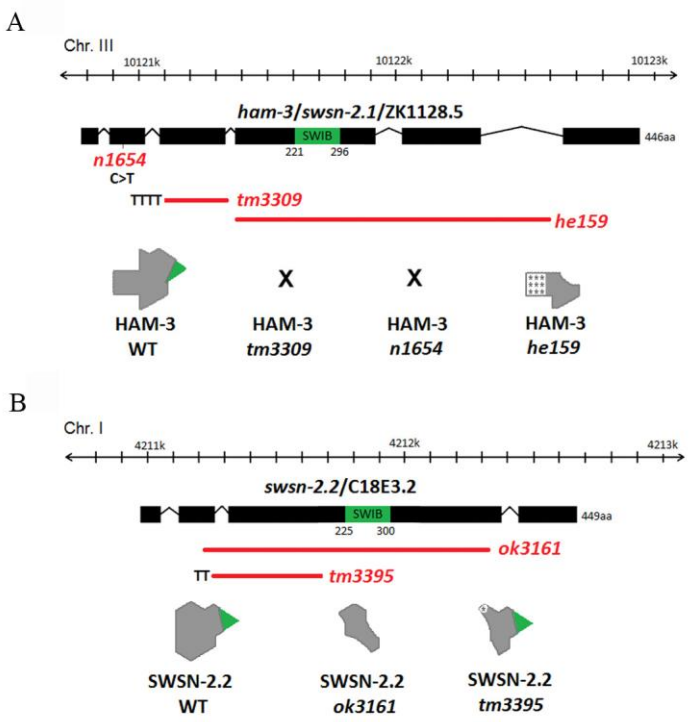

Figure 1 Scheme of *ham-3* and *swsn-2.2* mutant alleles and their expected gene products
The SWIB domain is labeled in green. Red bars represent deletions. Letters indicate insertions or transitions. In the drawing for the expected protein products, asterisks in the grey background indicate amino acids different from the original sequence.(A) *ham-3(n1654)* and *ham-3(tm3309)* are putative null alleles. *ham-3(he159)* encodes a truncated protein lacking the central SWIB domain. (B) Both *swsn-2.2* mutant alleles produce truncated proteins. While the product encoded by *swsn-2.2(ok3161)* lacks the central domain, *swsn-2.2(tm3395)* gives a chimeric protein containing the SWIB motif.

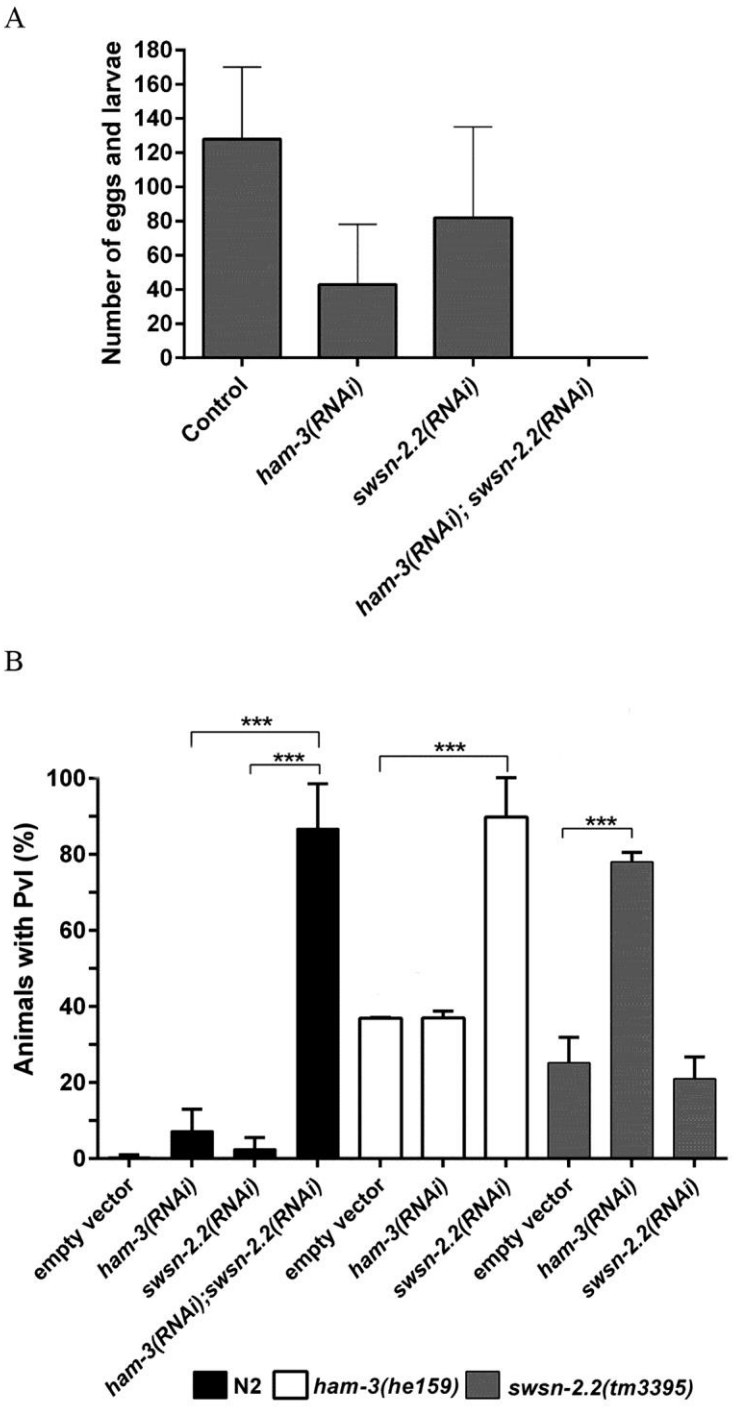

Figure 2. ***ham-3*** **and** ***swsn-2.2*** **act redundantly in fertility and vulva development**
(A) RNAi of *ham-3* or *swsn-2.2* causes reduced brood size, but double RNAi results in sterility. Synchronized L1 larvae (n≥24) were grown on the indicated RNAi plate at 25°C and their progeny was counted. Error bars indicate the standard deviations in the brood sizes determined in two independent experiments. (B) *ham-3* and *swsn-2.2* act redundantly in vulval induction. Wild type (N2) (n≥86) or mutants (n≥58) were seeded on the indicated RNAi plates at L1 stage. Experiments with N2 were performed at 25°C, the experiments with *ham-3* or *swsn-2.2* mutants at 20°C. The number of animals showing Pvl was determined at young adult stage. Error bars indicate the standard deviation between two independent experiments. The statistical significance was calculated with a two tailed student's t-test.
*** indicates a p value ≤ 0.001.

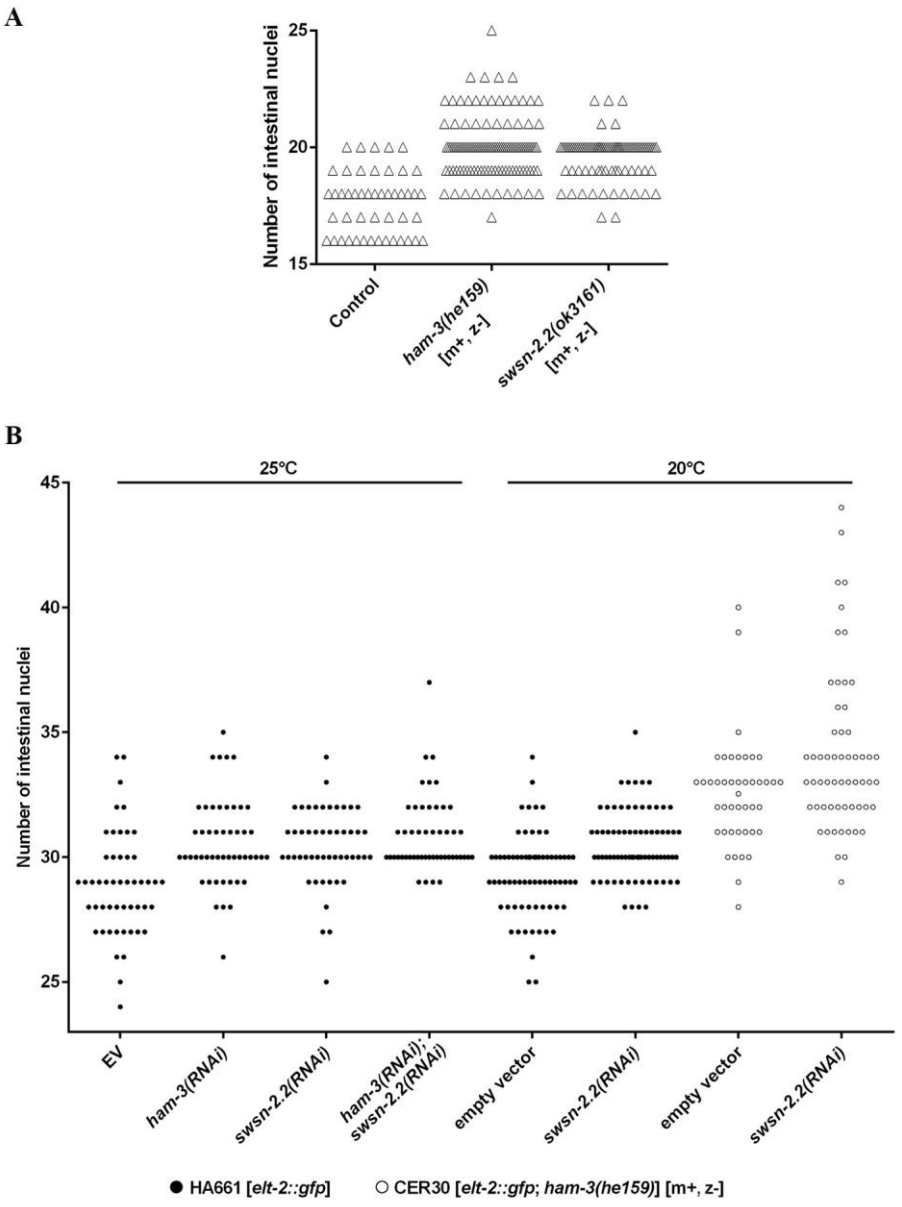

Figure 3. ***ham-3*** **and** ***swsn-2.2*** **regulate the number of intestinal nuclei**
(A) The number of intestinal nuclei of homozygous *ham-3(he159)* and *swsn-2.2(ok3161)* mutants bearing a P*elt-2::gfp* reporter was determined at L1 stage (n≥48). In both cases mutants came from heterozygous mothers [m+, z-] and were grown at 20°C. [m+ or m-] indicates maternal, [z+ or z-] zygotic contribution of the respective protein. (B) The number of GFP-positive intestinal nuclei was determined at L4 stage in *Pelt-2::gfp* animals (n≥44). Due to the sickness of *ham-3(he159)* mutants at high temperatures, experiments with this allele were performed at 20°C.

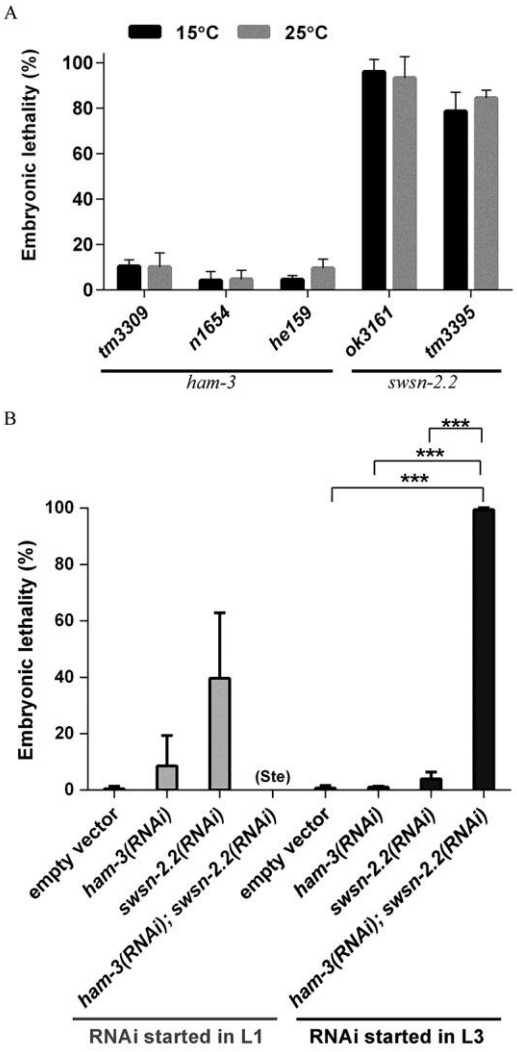

Figure 4. Embryonic lethality caused by RNAi and mutations of *ham-3* and *swsn-2.2*
(A) *swsn-2.2* mutants display higher embryonic lethality than *ham-3* mutants. Homozygote mutants (F1) were grown at 15°C until reaching the adult stage, dissected and the embryos (F2) incubated at the indicated temperatures. 24h after dissection, the numbers of eggs unable to hatch were determined (n≥371). Apart from *swsn-2.2(ok3161)* and *ham-3(tm3309),* all dissected animals derived from homozygote mothers (P0). (B) RNAi assays uncover a functional redundancy between *ham-3* and *swsn-2.2* in embryonic development. Starting the RNAi at L3 stage the animals fed with both RNAi clones bypassed the sterile phenotype, observed when RNAi starts at L1, and a synthetic embryonic phenotype was observed. Error bars indicate the standard deviation between two independent experimens. The statistical significance was calculated based on a two tailed student's t-test. *** indicates a p value ≤ 0.001.

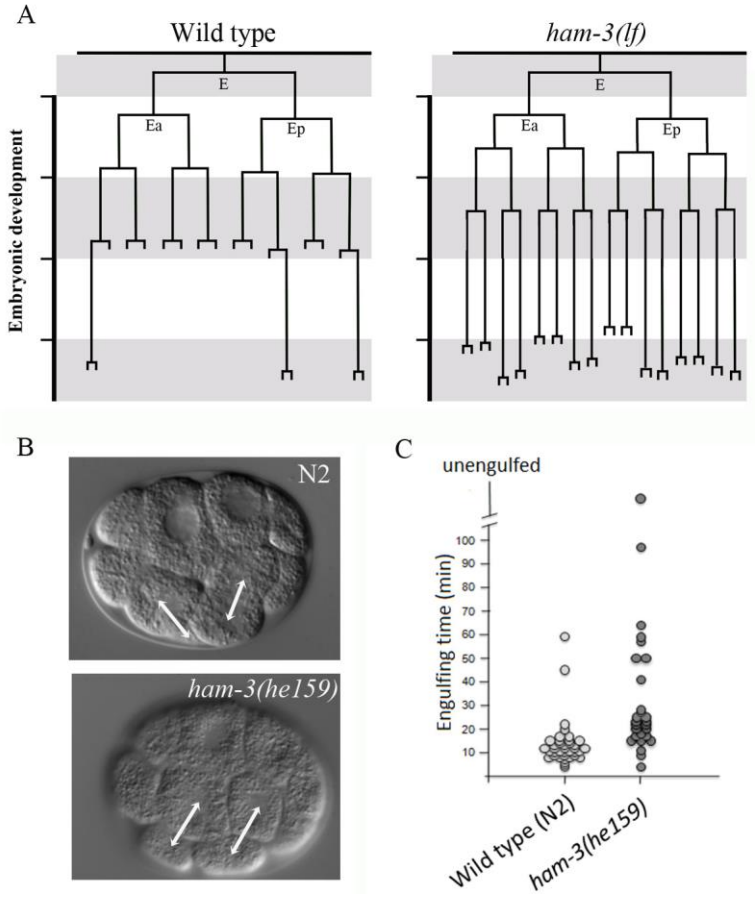

Figure 5. Embryonic phenotypes of *ham-3* mutants
(A) *ham-3(he159)* and *ham-3(n1654)* mutants (represented as *ham-3(lf)*) exhibit additional cell divisions in the E lineage. (B) *ham-3(he159)* embryo displaying an abnormal orientation of the mitotic spindle of the embryonic ABar cell. (C) *ham-3(he159)* embryos show a delay in the engulfment of apoptotic bodies.

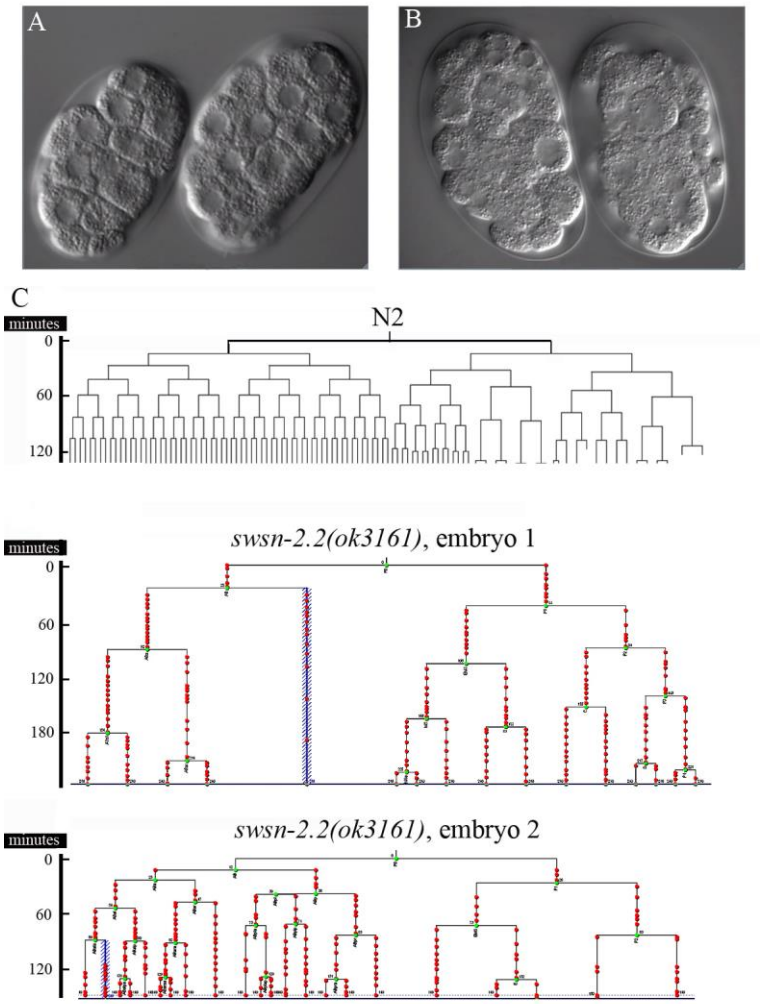

Figure 6 ***swsn-2.2*** **mutants present cell division defects in the early embryo**
(A) N2 wild type embryos after few rounds of cell division. The size of nuclei in each embryo is uniform. (B) Early *swsn-2.2(ok3161)* embryos show nuclei of different sizes, which are indicative of defective cell divisions. (C) Wild type embryonic cell lineage for the first cell divisions and cell lineages of two *swsn-2.2(ok3161)* embryos produced by homozygote mothers. Green and red spots indicate cell divisions and points of lineage scoring, respectively. The aberrant cell division pattern in *swsn-2.2(ok3161)* embryos hampers the lineage analysis after few divisions and causes the death of the embryos before comma stage.

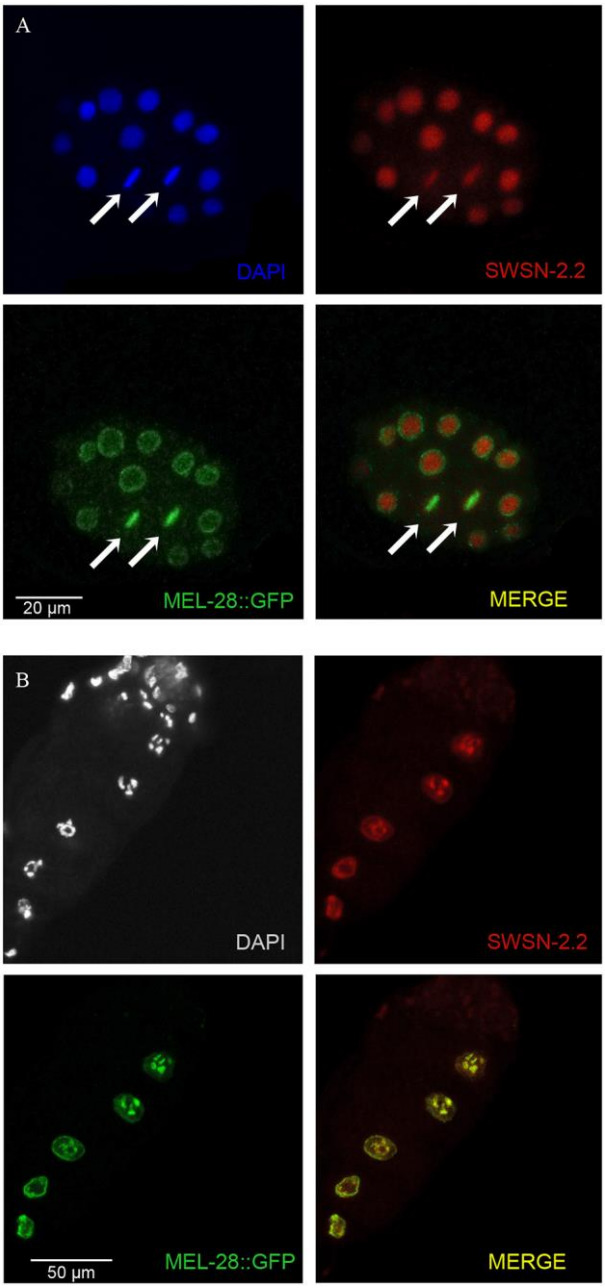

Figure 7 SWSN-2.2 and GFP::MEL-28 co-localize in early embryos and in oocytes
Immunofluorescence with anti-SWSN-2.2 and anti-GFP antibodies in transgenic animals expressing GFP::MEL-28. All images are the projection of three confocal sections of 1 µm. (A) Arrows indicate mitotic chromosomes of early embryonic cells. (B) SWSN-2.2 and GFP::MEL-28 co-localize in the nuclear membrane and in meiotic chromosomes of developing oocytes.

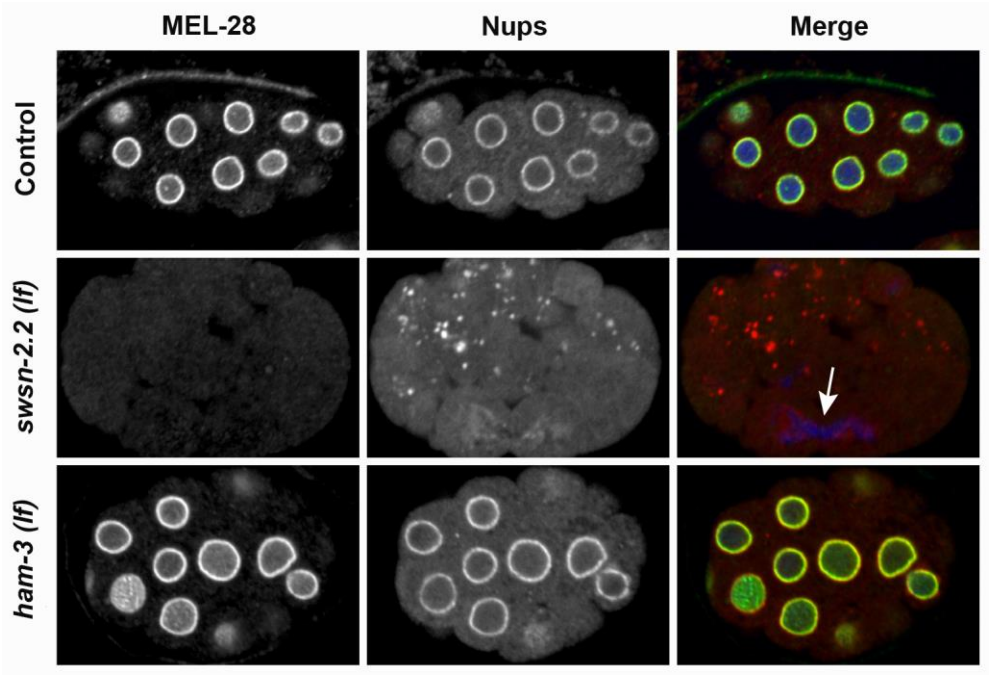

Figure 8 SWSN-2.2 is required for correct chromosome inheritance and post-mitotic nuclear reassembly in early embryos

Immunostaining with specific antibodies against MEL-28 and mAb414 against several nuclear pore proteins (Nups) in early *swsn-2.2(ok3161)* and *ham-3(he159)* embryos show distinct functions of HAM-3 and SWSN-2.2 in cell division. While absence of functional *swsn-2.2* impairs nuclear re-assembly and correct chromosome segregation, these processes are not affected by *ham-3(lf)*. In *swsn-2.2* mutants, MEL-28 signal is strongly reduced, whereas Nups accumulate in cytoplasmic aggregates. The arrow indicates chromatin trapped in a cleavage furrow.

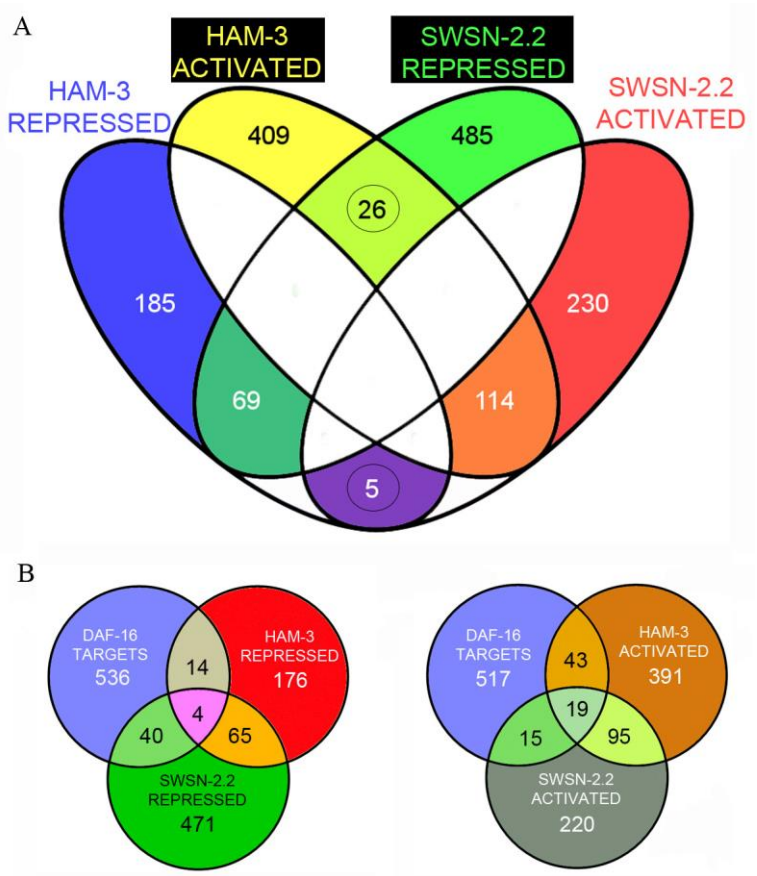

Figure 9. Transcriptomic analysis of *ham-3(RNAi)* and *swsn-2.2(RNAi)* animals
(A) Genes whose expression is activated or repressed by *ham-3* or *swsn-2.2*. L1 animals were fed for 36h at 25°C with *ham-3(RNAi)*, *swsn-2.2(RNAi)* or *gfp(RNAi)* as a control. The 31 genes that seem to be antagonistically regulated by *ham-3* and *swsn-2.2*, are not statistically significant (p≤0,96). The overlaps between genes activated and repressed by both genes were significant with p values ≤ 0,0001. Expression of five of these genes was analyzed by qPCR and we detected a differential rather than an antagonistic regulation (Figure S18). (B) HAM-3 and SWSN-2.2 targets significantly overlap with DAF-16 targets (p≤0,0001). A list of 594 genes regulated by DAF-16 was retrieved from Pinkston-Gosse J et al (PINKSTON-GOSSE and KENYON 2007) and compared with genes activated or repressed by HAM-3 or SWSN-2.2. Overlap significance was calculated with Chi-square tests with Yates' correction.

Table 1

Phenotype	Pvl (%)		Egl (%)		Adl (%)	
Temperature	**15°C**	**25°C**	**15°C**	**25°C**	**15°C**	**25°C**
***ham-3(tm3309)* [m+,z-]**	100	72.5	100	n.d. (Ste)	87.2	52
***ham-3(n1654)* [m-,z-]**	62.2	80.7	100	100	91.7	100
***ham-3(he159)* [m-,z-]**	59.9	100	100	100	80	90
***swsn-2.2(ok3161)* [m+,z-]**	89.3	91.6	37.5	45.8	11.1	50
***swsn-2.2(tm3395)* [m-,z-]**	58.7	95	0	6.25	35	35

Table 1. Temperature-dependence of some *ham-3* and *swsn-2.2* mutant phenotypes
To score the Protruding vulva (Pvl) phenotype, homozygote animals were grown at 15°C, gravid mothers dissected and the progeny incubated at the respective temperatures until reaching adult stage (n≥122). To investigate Egg-laying defects (Egl), homozygote animals were grown at 15°C until reaching L4 stage, singled out and incubated at the indicated temperatures. Mothers that accumulated embryos and/or died due to the Bag of worms (Bag) or Rupturing vulva (Rup) phenotypes were regarded as Egl (n≥30). Animals that died within 96h or 72h (at 15°C or 25°C, respectively) were scored as adult lethal (Adl).
[m+ or m-] indicates maternal, [z+ or z-] zygotic contribution of the respective wild type protein.

Protein	Function	Mixed stage (replicate 1)	Mixed stage (replicate 2)	Young adults
		#Peptides	#Peptides	#Peptides
SWSN-1	SWI/SNF subunit	11	16	35
SWSN-2.2	SWI/SNF subunit	6	10	12
SWSN-3	SWI/SNF subunit	1	5	13
SWSN-4	SWI/SNF subunit	0	4	13
SWSN-5 (SNFC-5)	SWI/SNF subunit	0	2	7
SWSN-6	SWI/SNF subunit	0	2	11
SWSN-7	SWI/SNF subunit	0	1	0
SWSN-8 (LET-526)	SWI/SNF subunit	0	0	15
SWSN-9	SWI/SNF subunit	0	0	4
PBRM-1	SWI/SNF subunit	0	0	3
PHF-10	SWI/SNF subunit	0	0	3
SAO-1	Early embryo	1	4	4
ATX-2	Early embryo	0	3	6
NPP-2	Nuclear envelope	0	1	0
NPP-9, isoform a	Nuclear envelope	2	1	0
MEL-28	Nuclear envelope	1	0	0
HUM-5	Myosin-related	10	0	0
HUM-2	Myosin-related	2	0	0
MLC-6	Myosin-related	3	1	0
MLC-7	Myosin-related	4	0	0
TNT-4	Myosin-related	4	0	0
C30H6.7	Acetyltransferase	7	4	3
TAF-9	Transcription	1	1	1
ZK973.9	Arp2/3 complex	0	2	2

Table 2. Some of the proteins identified as interactors of SWSN-2.2 by Co-Immunoprecipitation and Mass spectrometry. This table lists some of the SWSN-2.2 interactors identified. The full list is available as supplementary table (Table S1). While the first two replicates were performed with mixed developmental stages, a synchronized population of young adults was used for the third experiment. The total number of interactors identified was 64 (mixed stage, replicate 1), 57 (mixed stage, replicate 2), and 99 (young adult stage).

SUPPORTING INFORMATION

Supplementary Figures – File containing supporting Figures S1 to S18.

Supplementary Table 1 – SWSN-2.2 interactors resulting from proteomic analyses

Supplementary Table 2 - Genes up- and down-regulated in *ham-3(RNAi)* and *swsn-2.2(RNAi)* animals.

Supplementary File S1 – Movie: cellular divisions in a wild-type early embryo

Supplementary File S2 - Movie: cellular divisions in a *swsn-2.2(ok3161)* early embryo

Supplementary File S3 – Movie: wild-type embryo development (to later stage and faster motion than S1)

Supplementary File S4 - Movie: *swsn-2.2(ok3161)* embryo development (to later stage and faster motion than S2)

REFERENCES

ANDERSEN E. C., SAFFER A. M., HORVITZ H. R., 2008 Multiple levels of redundant processes inhibit Caenorhabditis elegans vulval cell fates. Genetics **179**: 2001–12.

ASKJAER P., GALY V., MEISTER P., 2014 Modern tools to study nuclear pore complexes and nucleocytoplasmic transport in Caenorhabditis elegans. Methods Cell Biol. **122**: 277–310.

BERDASCO M., ESTELLER M., 2013 Genetic syndromes caused by mutations in epigenetic genes. Hum. Genet. **132**: 359–83.

BEZHANI S., WINTER C., HERSHMAN S., WAGNER J. D., KENNEDY J. F., KWON C. S., PFLUGER J., SU Y., WAGNER D., 2007 Unique, shared, and redundant roles for the Arabidopsis SWI/SNF chromatin remodeling ATPases BRAHMA and SPLAYED. Plant Cell **19**: 403–16.

CABELLO J., NEUKOMM L. J., GÜNESDOGAN U., BURKART K., CHARETTE S. J., LOCHNIT G., HENGARTNER M. O., SCHNABEL R., 2010 The Wnt pathway controls cell death engulfment, spindle orientation, and migration through CED-10/Rac. PLoS Biol. **8**: e1000297.

CEOL C. J., STEGMEIER F., HARRISON M. M., HORVITZ H. R., 2006 Identification and classification of genes that act antagonistically to let-60 Ras signaling in Caenorhabditis elegans vulval development. Genetics **173**: 709–26.

CERON J., RUAL J.-F., CHANDRA A., DUPUY D., VIDAL M., HEUVEL S. VAN DEN, 2007 Large-scale RNAi screens identify novel genes that interact with the C. elegans retinoblastoma pathway as well as splicing-related components with synMuv B activity. BMC Dev. Biol. **7**: 30.

CLUCAS C., CABELLO J., BÜSSING I., SCHNABEL R., JOHNSTONE I. L., 2002 Oncogenic potential of a C.elegans cdc25 gene is demonstrated by a gain-of-function allele. EMBO J. **21**: 665–74.

CUI M., FAY D. S., HAN M., 2004 lin-35/Rb cooperates with the SWI/SNF complex to control Caenorhabditis elegans larval development. Genetics **167**: 1177–85.

DESAI C., GARRIGA G., MCINTIRE S. L., HORVITZ H. R., 1988 A genetic pathway for the development of the Caenorhabditis elegans HSN motor neurons. Nature **336**: 638–46.

EUSKIRCHEN G. M., AUERBACH R. K., DAVIDOV E., GIANOULIS T. A., ZHONG G., ROZOWSKY J., BHARDWAJ N., GERSTEIN M. B., SNYDER M., 2011 Diverse roles and interactions of the SWI/SNF chromatin remodeling complex revealed using global approaches. PLoS Genet. **7**: e1002008.

EUSKIRCHEN G., AUERBACH R. K., SNYDER M., 2012 SWI/SNF chromatin-remodeling factors: multiscale analyses and diverse functions. J. Biol. Chem. **287**: 30897–905.

FAY D. S., YOCHEM J., 2007 The SynMuv genes of Caenorhabditis elegans in vulval development and beyond. Dev. Biol. **306**: 1–9.

FERNANDEZ A. G., MIS E. K., LAI A., MAURO M., QUENTAL A., BOCK C., PIANO F., 2014 Uncovering buffered pleiotropy: a genome-scale screen for mel-28 genetic interactors in Caenorhabditis elegans. G3 (Bethesda). **4**: 185–96.

FERNANDEZ A. G., PIANO F., 2006 MEL-28 is downstream of the Ran cycle and is required for nuclear-envelope function and chromatin maintenance. Curr. Biol. **16**: 1757–63.

FONTRODONA L., PORTA-DE-LA-RIVA M., MORÁN T., NIU W., DÍAZ M., ARISTIZÁBAL-CORRALES D., VILLANUEVA A., SCHWARTZ S., REINKE V., CERÓN J., 2013 RSR-2, the Caenorhabditis elegans ortholog of human spliceosomal component SRm300/SRRM2, regulates development by influencing the transcriptional machinery. (N Maizels, Ed.). PLoS Genet. **9**: e1003543.

FORCALES S. V, ALBINI S., GIORDANI L., MALECOVA B., CIGNOLO L., CHERNOV A., COUTINHO P., SACCONE V., CONSALVI S., WILLIAMS R., WANG K., WU Z., BARANOVSKAYA S., MILLER A., DILWORTH F. J., PURI P. L., 2012 Signal-dependent incorporation of MyoD-BAF60c into Brg1-based SWI/SNF chromatin-remodelling complex. EMBO J. **31**: 301–16.

FRØKJÆR-JENSEN C., 2013 Exciting prospects for precise engineering of Caenorhabditis elegans genomes with CRISPR/Cas9. Genetics **195**: 635–42.

FUJITA M., TAKESHITA H., SAWA H., 2007 Cyclin E and CDK2 repress the terminal differentiation of quiescent cells after asymmetric division in C. elegans. PLoS One **2**: e407.

GALY V., ASKJAER P., FRANZ C., LÓPEZ-IGLESIAS C., MATTAJ I. W., 2006 MEL-28, a novel nuclear-envelope and kinetochore protein essential for zygotic nuclear-envelope assembly in C. elegans. Curr. Biol. **16**: 1748–56.

GALY V., MATTAJ I. W., ASKJAER P., 2003 Caenorhabditis elegans nucleoporins Nup93 and Nup205 determine the limit of nuclear pore complex size exclusion in vivo. Mol. Biol. Cell **14**: 5104–15.

GÓMEZ-ORTE E., SÁENZ-NARCISO B., MORENO S., CABELLO J., 2013 Multiple functions of the noncanonical Wnt pathway. Trends Genet. **29**: 545–53.

GUPTA B. P., HANNA-ROSE W., STERNBERG P. W., 2012 Morphogenesis of the vulva and the vulval-uterine connection. WormBook: 1–20.

HALE V. A., GUINEY E. L., GOLDBERG L. Y., HADUONG J. H., KWARTLER C. S., SCANGOS K. W., GOUTTE C., 2012 Notch signaling is antagonized by SAO-1, a novel GYF-domain protein that interacts with the E3 ubiquitin ligase SEL-10 in Caenorhabditis elegans. Genetics **190**: 1043–57.

HARGREAVES D. C., CRABTREE G. R., 2011 ATP-dependent chromatin remodeling: genetics, genomics and mechanisms. Cell Res. **21**: 396–420.

HAYES G. D., RIEDEL C. G., RUVKUN G., 2011 The Caenorhabditis elegans SOMI-1 zinc finger protein and SWI/SNF promote regulation of development by the mir-84 microRNA. Genes Dev. **25**: 2079–92.

HELMING K. C., WANG X., ROBERTS C. W. M., 2014 Vulnerabilities of mutant SWI/SNF complexes in cancer. Cancer Cell **26**: 309–17.

HERMAN M. A., 2002 Control of cell polarity by noncanonical Wnt signaling in C. elegans. Semin. Cell Dev. Biol. **13**: 233–41.

HO L., CRABTREE G. R., 2010 Chromatin remodelling during development. Nature **463**: 474–84.

HO L., RONAN J. L., WU J., STAAHL B. T., CHEN L., KUO A., LESSARD J., NESVIZHSKII A. I., RANISH J., CRABTREE G. R., 2009 An embryonic stem cell chromatin remodeling complex, esBAF, is essential for embryonic stem cell self-renewal and pluripotency. Proc. Natl. Acad. Sci. U. S. A. **106**: 5181–6.

HOLSTEGE F. C., JENNINGS E. G., WYRICK J. J., LEE T. I., HENGARTNER C. J., GREEN M. R., GOLUB T. R., LANDER E. S., YOUNG R. A., 1998 Dissecting the regulatory circuitry of a eukaryotic genome. Cell **95**: 717–28.

IMBALZANO A. N., IMBALZANO K. M., NICKERSON J. A., 2013 BRG1, a SWI/SNF chromatin remodeling enzyme ATPase, is required for maintenance of nuclear shape and integrity. Commun. Integr. Biol. **6**: e25153.

INOUE T., SHERWOOD D. R., ASPÖCK G., BUTLER J. A., GUPTA B. P., KIROUAC M., WANG M., LEE P.-Y., KRAMER J. M., HOPE I., BÜRGLIN T. R., STERNBERG P. W., 2002 Gene expression markers for Caenorhabditis elegans vulval cells. Mech. Dev. **119 Suppl** : S203–9.

JENSEN V. L., SIMONSEN K. T., LEE Y.-H., PARK D., RIDDLE D. L., 2010 RNAi screen of DAF-16/FOXO target genes in C. elegans links pathogenesis and dauer formation. PLoS One **5**: e15902.

JORDAN N. V., PRAT A., ABELL A. N., ZAWISTOWSKI J. S., SCIAKY N., KARGINOVA O. A., ZHOU B., GOLITZ B. T., PEROU C. M., JOHNSON G. L., 2013 SWI/SNF chromatin-remodeling factor Smarcd3/Baf60c controls epithelial-mesenchymal transition by inducing Wnt5a signaling. Mol. Cell. Biol. **33**: 3011–25.

KAMATH R. S., FRASER A. G., DONG Y., POULIN G., DURBIN R., GOTTA M., KANAPIN A., BOT N. LE, MORENO S., SOHRMANN M., WELCHMAN D. P., ZIPPERLEN P., AHRINGER J., 2003 Systematic functional analysis of the Caenorhabditis elegans genome using RNAi. Nature **421**: 231–7.

KIEHL T.-R., SHIBATA H., PULST S.-M., 2000 The Ortholog of Human Ataxin-2 is Essential for Early Embryonic Patterning in C. elegans. J. Mol. Neurosci. **15**: 231–242.

KIMBLE J., CRITTENDEN S. L., 2005 Germline proliferation and its control. WormBook: 1–14.

KORTA D. Z., HUBBARD E. J. A., 2010 Soma-germline interactions that influence germline proliferation in Caenorhabditis elegans. Dev. Dyn. **239**: 1449–59.

KOSTIĆ I., LI S., ROY R., 2003 cki-1 links cell division and cell fate acquisition in the C. elegans somatic gonad. Dev. Biol. **263**: 242–52.

KOSTIĆ I., ROY R., 2002 Organ-specific cell division abnormalities caused by mutation in a general cell cycle regulator in C. elegans. Development **129**: 2155–65.

KRÜGER A. V, JELIER R., DZYUBACHYK O., ZIMMERMAN T., MEIJERING E., LEHNER B., 2014 Comprehensive single cell-resolution analysis of the role of chromatin regulators in early C. elegans embryogenesis. Dev. Biol.

KUZMANOV A., KARINA E. I., KIRIENKO N. V, FAY D. S., 2014 The conserved PBAF nucleosome-remodeling complex mediates the response to stress in Caenorhabditis elegans. Mol. Cell. Biol. **34**: 1121–35.

LANS H., MARTEIJN J. a, SCHUMACHER B., HOEIJMAKERS J. H. J., JANSEN G., VERMEULEN W., 2010 Involvement of global genome repair, transcription coupled repair, and chromatin remodeling in UV DNA damage response changes during development. PLoS Genet. **6**: e1000941.

LARGE E. E., MATHIES L. D., 2014 Caenorhabditis elegans SWI/SNF subunits control sequential developmental stages in the somatic gonad. G3 (Bethesda). **4**: 471–83.

MASLIAH-PLANCHON J., BIÈCHE I., GUINEBRETIÈRE J.-M., BOURDEAUT F., DELATTRE O., 2014 SWI/SNF Chromatin Remodeling and Human Malignancies. Annu. Rev. Pathol. Mech. Dis. **10**: 141111110736006.

MATTOUT A., CABIANCA D. S., GASSER S. M., 2015 Chromatin states and nuclear organization in development — a view from the nuclear lamina. Genome Biol. **16**: 174.

McCarter J., Bartlett B., Dang T., Schedl T., 1997 Soma-germ cell interactions in Caenorhabditis elegans: multiple events of hermaphrodite germline development require the somatic sheath and spermathecal lineages. Dev. Biol. **181**: 121–43.

Michaelson D., Korta D. Z., Capua Y., Hubbard E. J. A., 2010 Insulin signaling promotes germline proliferation in C. elegans. Development **137**: 671–80.

Narlikar G. J., Sundaramoorthy R., Owen-Hughes T., 2013 Mechanisms and functions of ATP-dependent chromatin-remodeling enzymes. Cell **154**: 490–503.

Nieto C., Almendinger J., Gysi S., Gómez-Orte E., Kaech A., Hengartner M. O., Schnabel R., Moreno S., Cabello J., 2010 ccz-1 mediates the digestion of apoptotic corpses in C. elegans. J. Cell Sci. **123**: 2001–7.

Oh J., Sohn D. H., Ko M., Chung H., Jeon S. H., Seong R. H., 2008 BAF60a interacts with p53 to recruit the SWI/SNF complex. J. Biol. Chem. **283**: 11924–34.

Phelan M. L., Sif S., Narlikar G. J., Kingston R. E., 1999 Reconstitution of a core chromatin remodeling complex from SWI/SNF subunits. Mol. Cell **3**: 247–53.

Pinkston-Gosse J., Kenyon C., 2007 DAF-16/FOXO targets genes that regulate tumor growth in Caenorhabditis elegans. Nat. Genet. **39**: 1403–9.

Puri P. L., Mercola M., 2012 BAF60 A, B, and Cs of muscle determination and renewal. Genes Dev. **26**: 2673–83.

Qi W., Huang X., Neumann-Haefelin E., Schulze E., Baumeister R., 2012 Cell-nonautonomous signaling of FOXO/DAF-16 to the stem cells of Caenorhabditis elegans. PLoS Genet. **8**: e1002836.

Reisman D., Glaros S., Thompson E. A., 2009 The SWI/SNF complex and cancer. Oncogene **28**: 1653–68.

Riedel C. G., Dowen R. H., Lourenco G. F., Kirienko N. V, Heimbucher T., West J. A., Bowman S. K., Kingston R. E., Dillin A., Asara J. M., Ruvkun G., 2013 DAF-16 employs the chromatin remodeller SWI/SNF to promote stress resistance and longevity. Nat. Cell Biol. **15**: 491–501.

Rocheleau C. E., Downs W. D., Lin R., Wittmann C., Bei Y., Cha Y. H., Ali M., Priess J. R., Mello C. C., 1997 Wnt signaling and an APC-related gene specify endoderm in early C. elegans embryos. Cell **90**: 707–16.

Romero O. A., Sanchez-Cespedes M., 2014 The SWI/SNF genetic blockade: effects in cell differentiation, cancer and developmental diseases. Oncogene **33**: 2681–9.

Rual J.-F., Ceron J., Koreth J., Hao T., Nicot A.-S., Hirozane-Kishikawa T., Vandenhaute J., Orkin S. H., Hill D. E., Heuvel S. van den, Vidal M., 2004 Toward improving Caenorhabditis elegans phenome mapping with an ORFeome-based RNAi library. Genome Res. **14**: 2162–8.

Ruijtenberg S., van den Heuvel S., 2015 G1/S Inhibitors and the SWI/SNF Complex Control Cell-Cycle Exit during Muscle Differentiation. Cell **162**: 300–313.

Santen G. W. E., Kriek M., Attikum H. van, 2012 SWI/SNF complex in disorder: SWItching from malignancies to intellectual disability. Epigenetics **7**: 1219–24.

Sarshad A., Sadeghifar F., Louvet E., Mori R., Böhm S., Al-Muzzaini B., Vintermist A., Fomproix N., Östlund A.-K., Percipalle P., 2013 Nuclear myosin 1c facilitates the chromatin

modifications required to activate rRNA gene transcription and cell cycle progression. PLoS Genet. **9**: e1003397.

SAWA H., KOUIKE H., OKANO H., 2000 Components of the SWI/SNF complex are required for asymmetric cell division in C. elegans. Mol. Cell **6**: 617–24.

SHAIN a H., POLLACK J. R., 2013 The spectrum of SWI/SNF mutations, ubiquitous in human cancers. PLoS One **8**: e55119.

SHIBATA Y., UCHIDA M., TAKESHITA H., NISHIWAKI K., SAWA H., 2012 Multiple functions of PBRM-1/Polybromo- and LET-526/Osa-containing chromatin remodeling complexes in C. elegans development. Dev. Biol. **361**: 349–57.

STERNBERG P. W., 2005 Vulval development. WormBook: 1–28.

STERNBERG P. W., HAN M., 1998 Genetics of RAS signaling in C. elegans. Trends Genet. **14**: 466–72.

SULSTON J. E., SCHIERENBERG E., WHITE J. G., THOMSON J. N., 1983 The embryonic cell lineage of the nematode Caenorhabditis elegans. Dev. Biol. **100**: 64–119.

TRAPNELL C., ROBERTS A., GOFF L., PERTEA G., KIM D., KELLEY D. R., PIMENTEL H., SALZBERG S. L., RINN J. L., PACHTER L., 2012 Differential gene and transcript expression analysis of RNA-seq experiments with TopHat and Cufflinks. Nat. Protoc. **7**: 562–78.

WATANABE R., UI A., KANNO S.-I., OGIWARA H., NAGASE T., KOHNO T., YASUI A., 2014 SWI/SNF factors required for cellular resistance to DNA damage include ARID1A and ARID1B and show interdependent protein stability. Cancer Res. **74**: 2465–75.

WEINBERG P., FLAMES N., SAWA H., GARRIGA G., HOBERT O., 2013 The SWI/SNF Chromatin Remodeling Complex Selectively Affects Multiple Aspects of Serotonergic Neuron Differentiation. Genetics.

WEISSMAN B., KNUDSEN K. E., 2009 Hijacking the chromatin remodeling machinery: impact of SWI/SNF perturbations in cancer. Cancer Res. **69**: 8223–30.

WOOLNER S., BEMENT W. M., 2009 Unconventional myosins acting unconventionally. Trends Cell Biol. **19**: 245–52.

YOO A. S., BAIS C., GREENWALD I., 2004 Crosstalk between the EGFR and LIN-12/Notch pathways in C. elegans vulval development. Science **303**: 663–6.